A novel knockout mouse model to assess the impact of one-copy loss of Hnrnpk in CD4+T cells in chronically inflamed skin as a prelude to CTCL

Luo, Y.X.; Vermeer, M.; Linssen, M.M.; Bie, F.J. de; Pijnacker-Verspuij, M.; Brouwers, C.; ... ; Tensen, C.P.

scientific reports

Check for updates

OPEN

A novel knockout mouse model to assess the impact of one-copy loss of *Hnrnpk* in CD4 + T cells in chronically inflamed skin as a prelude to CTCL

Yixin Luo[1], Maarten Vermeer[1], Margot M. Linssen[2], Fenna J. de Bie[1], Marloe Pijnacker-Verspuij[3], Conny Brouwers[2], Jill Claassens[2], Frank R. de Gruijl[1], Peter Hohenstein[2] & Cornelis P. Tensen[1]✉

Cutaneous T-cell lymphomas (CTCLs), particularly Mycosis fungoides (MF), frequently exhibit deletions and reduced expression of *HNRNPK* in CD4 + T cells. To enable in vivo studies, we developed a conditional Hnrnpk knockout mouse that thrives, facilitating the investigation of *HNRNPK*'s role in CTCL onset. We generated mice with a floxed *Hnrnpk* allele, then crossbred them with *Cd4CreER*^{T2} mice to generate *Hnrnpk flox Cd4CreER*^{T2} mice, all in BL6 background. PCR confirmed the targeted deletion of *Hnrnpk* in CD4 + T cells after tamoxifen i.p. injection. Skin allergic reactions were induced with oxazolone, and Cre was activated in skin-infiltrating CD4 + T cells using tamoxifen topically after the first allergic skin reaction. The mice exhibited no immediately obvious phenotype. Flow cytometry and histopathological analysis were conducted on blood and skin samples collected throughout the experiment. Following 20 weeks of sustained allergic reactions, inflammation persisted over 20 weeks after challenges ceased, demonstrating early CTCL characteristics such as chronic skin inflammation, CD3 + CD4 + T cell infiltration, and stable peripheral blood parameters. This mouse model provides experimental access to the complex microenvironment and immune responses involved in early inflammatory stages, providing opportunities for further research into the role of *HNRNPK* in CTCL and the development of effective therapeutic interventions for this challenging malignancy.

Keywords Cutaneous T-cell lymphomas, Mycosis fungoides, CD4 + T cells, *HNRNPK*, Transgenic mouse

Abbreviations

4OHT	4-Hydroxy-Tamoxifen
ARRIVE	Animal research: Reporting of in vivo experiments
CCD	Central committee on animal experiments
CRISPR/Cas9	Clustered regularly interspaced short palindromic repeats/Cas9
CTCL	Cutaneous T-cell lymphomas
GEMMs	Genetically engineered mouse models
HE	Hematoxylin and eosin
HPF	High-power fields
HNRNPK	Heterogeneous nuclear ribonucleoprotein K
IHC	Immunohistochemistry
IvD	Animal welfare committee
LUMC	Leiden university medical center
MF	Mycosis fungoides
NHL	Non-Hodgkin's lymphomas
OXA	Oxazolone

[1]Department of Dermatology, Leiden University Medical Center, Leiden, The Netherlands. [2]Transgenic Facility Leiden, Central Animal Facility, Leiden University Medical Center, Leiden, The Netherlands. [3]Experimental Animal Facility, Leiden University Medical Center, Leiden, The Netherlands. ✉email: C.P.Tensen@lumc.nl

PCR	Polymerase chain reaction
SOCS1	Suppressor of cytokine signaling 1
ssODN	Single-stranded oligodeoxynucleotides
TAM	Tamoxifen

Cutaneous T-cell lymphomas (CTCL) are a diverse group of non-Hodgkin's lymphomas (NHL) characterized by the localization of neoplastic T lymphocytes to the skin[1,2]. Recent advancements have significantly contributed to our understanding of the molecular mechanisms underlying CTCL, revealing the involvement of genes such as heterogenous nuclear ribonucleoprotein K (*HNRNPK)* and Suppressor of cytokine signaling 1(*SOCS1)*[3–5]. However, a comprehensive understanding of CTCL requires the development of appropriate model systems that can capture the complex nature of the disease and facilitate the identification of effective therapeutic strategies[6].

The role of the tumor microenvironment within the lesions in the development, progression and treatment resistance of CTCL has become an important area of research due to its complicated pathogenesis[7]. In vitro models, although valuable, have limitations in simulating essential factors such as the tumor microenvironment and intact immune system, emphasizing the need for in vivo models[8–10]. Therefore, more sophisticated tools, such as genetically engineered mouse models, are indispensable for comprehensively exploring T-cell malignancies.

HNRNPK, a DNA and RNA-binding protein, regulates numerous cellular processes through transcriptional, posttranscriptional, and translational mechanisms[11,12]. Notably, its oncogenic and tumor-suppressive functions are context-dependent. Both overexpression and abnormally low expression of *HNRNPK* can be pathogenic, likely due to the dysregulation of multiple cellular oncogenes or tumor suppressor genes[13]. In the context of hematological malignancies, it has been observed that a 9q21.32 deletion encompassing the *HNRNPK* gene occurs in acute myeloid leukemia patients, resulting in the loss of one copy of *HNRNPK*[14,15]. Interestingly, the recurrent deletion of *HNRNPK* has been reported in mycosis fungoides (MF) and other CTCL subtypes[16,17]. Therefore, there is a compelling need to establish a CD4 + T-cell-specific murine model of *Hnrnpk* that accurately represents the intact immune system and tumor microenvironment. Such a model would be pivotal in elucidating the intricate and multifaceted role of *HNRNPK* in CTCL, ultimately leading to a better understanding of the disease and developing more effective therapeutic interventions.

This work describes a novel *Hnrnpk* mouse model designed based on the CTCL gene sequencing results. Here, we primarily wanted to examine the basic impact of Hnrnpk-ko limited to CD4 + T cells in an inflamed skin site on subsequent chronic (allergic) inflammation at this site as suspected prelude to CTCL. In this mouse model, the immune homeostasis in peripheral blood remains relatively undisturbed under chronic antigen exposure, while T-cell infiltration is confined to the skin. The skin lesions predominantly exhibit lymphocytic infiltration characterized by CD3 + CD4 + cells, and the infiltration persists without regression, aligning with early-stage CTCL characteristics.

Result

1. Generation of *Hnrnpk* flox and *Hnrnpk* flox *Cd4CreER*^{T2} mice.

To generate conditional knockout *Hnrnpk* mice, we employed CRISPR/Cas9 RNPs and 200 bp single-stranded oligodeoxynucleotides (ssODN) to sequentially target intron 2 and in the resulting mouse intron 6 of the *Hnrnpk* gene, in murine oocytes on C57BL/J background We designed the 5' ssODN (for intron 2) with a LoxP site, and introduced it into oocytes along with the CRISPR/Cas9 RNP complex.(Fig. 1A) Additionally, we designed the 3' ssODN (for intron 6) with a LoxP site and 3' HA, and introduced it into the resulting mouse line to target the LoxP site in intron 6. (Fig. 1B) (gRNA, ssODN listed in Table S1).

We screened the offspring for the correct insertion of the LoxP sites on genomic DNA from ear-clip biopsies by PCR and Sanger Sequencing. (Fig. 1C, D and E) (Original gel is presented in Supplementary Fig. 1). (Primers listed in Table S2) To confirm correct integration loxP site in intron 6, TOPO-TA PCR product subcloning was performed. As shown in Fig. 1F, the *Hnrnpk* flox mice were inserted with two loxP sites flanking exon 3 to 5. We bred these conditional mice to homozygosity and the offspring are healthy.

2. *Hnrnpk* knockout in CD4 + T cells confirmation.

To induce *Hnrnpk* knockout in CD4 + T cells, we crossed *Cd4CreER*^{T2} mice with *Hnrnpk* flox mice. Details of the cross-breeding scheme can be found in Fig. 2A. In *Cd4CreER*^{T2} mice, Cre recombinase is controlled by the Cd4 gene promoter and can be induced by tamoxifen. Homozygous *Hnrnpk flox* (*Hnrnpk* fl/fl) mice were crossed with the transgenic mice expressing Cre recombinase under the control of the Cd4 promoter (*Cd4CreER*^{T2} mice) to yield heterozygous littermates with the *Cd4CreER*^{T2} transgene. Offspring inherited both the targeted *Hnrnpk* fl/wt allele and the *Cd4CreER*^{T2} transgene.

In *Hnrnpk flox Cd4CreER*^{T2} mice, tamoxifen can selectively knock out *Hnrnpk* in CD4 + T cells. After five consecutive days of intraperitoneal tamoxifen injections in *Hnrnpk fl/wt Cd4CreER*^{T2} mice, splenocytes were collected and CD4 + T cells were enriched. (Fig. 2B) Flow cytometry analysis showed that CD4 + T cells accounted for approximately 94.1% after enrichment. (Fig. 2C). DNA was extracted from the enriched CD4 + T cells. Successful *Hnrnpk* deletion in CD4 + T cells of *Hnrnpk flox Cd4CreER*^{T2} mice treated with tamoxifen was confirmed through PCR analysis (primers listed in Table S3) showing the recombinant *Hnrnpk* (*Hnrnpk* KO). In contrast, the spleen CD4 + T cells enriched from mice not receiving tamoxifen injections showed no recombinant gene fragments following *Hnrnpk* deletion (*Hnrnpk* WT). (Fig. 2D) (Original gel is presented in Supplementary Fig. 2).

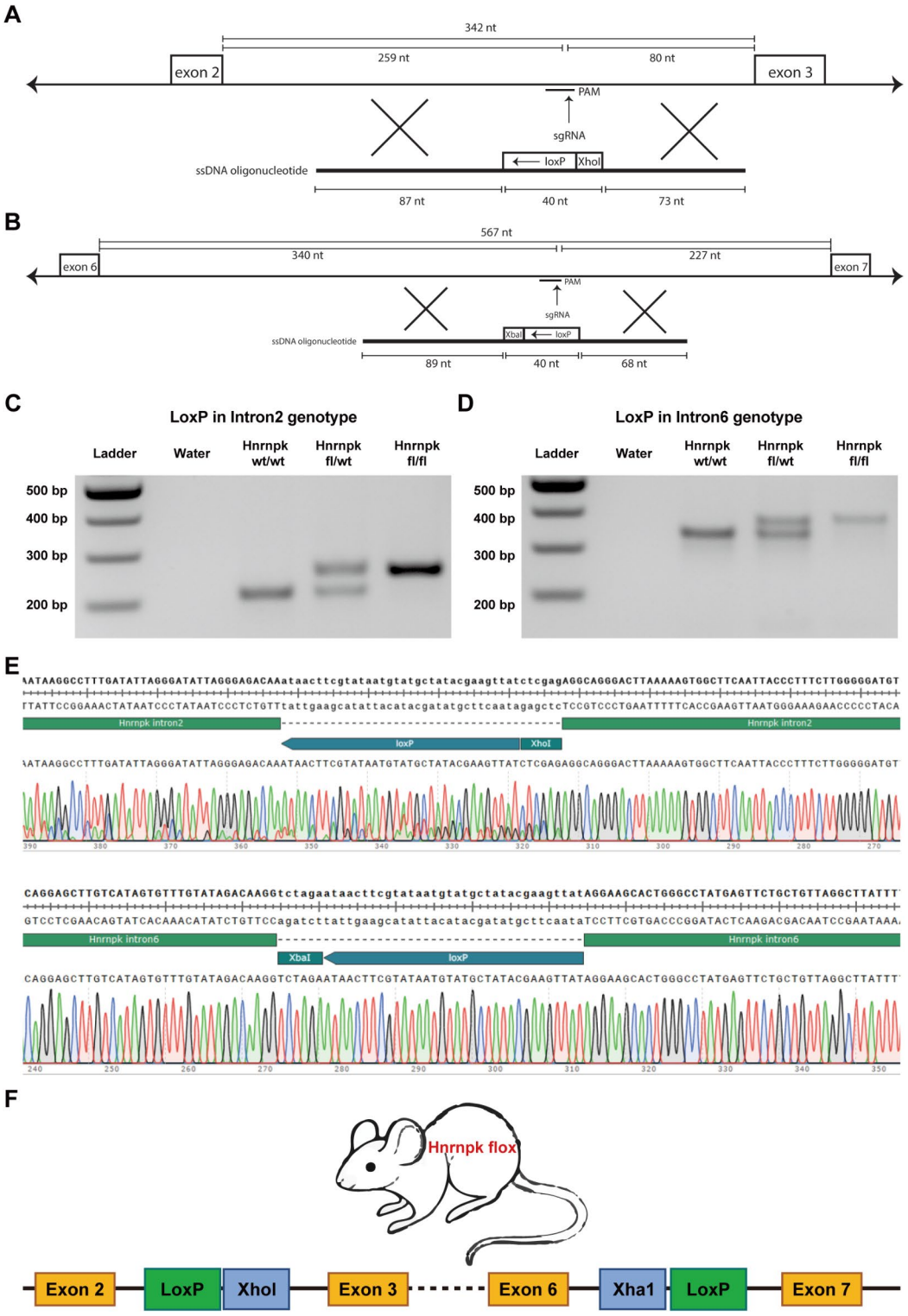

Fig. 1. (**A**, **B**) The structure of designed single-stranded oligodeoxynucleotides (ssODN) for intron 2 and intron 6 of *Hnrnpk*. (**C**, **D**) Agarose gel electrophoresis image showing the PCR product of LoxP inserted in intron 2 and intron 6 of *Hnrnpk*. (Original gel is presented in Supplementary Fig. 1). (**E**) Sanger sequencing chromatogram of both modifications. (**F**) The structure of the *Hnrnpk* flox modified gene with two LoxP sites in *Hnrnpk* flox mouse.

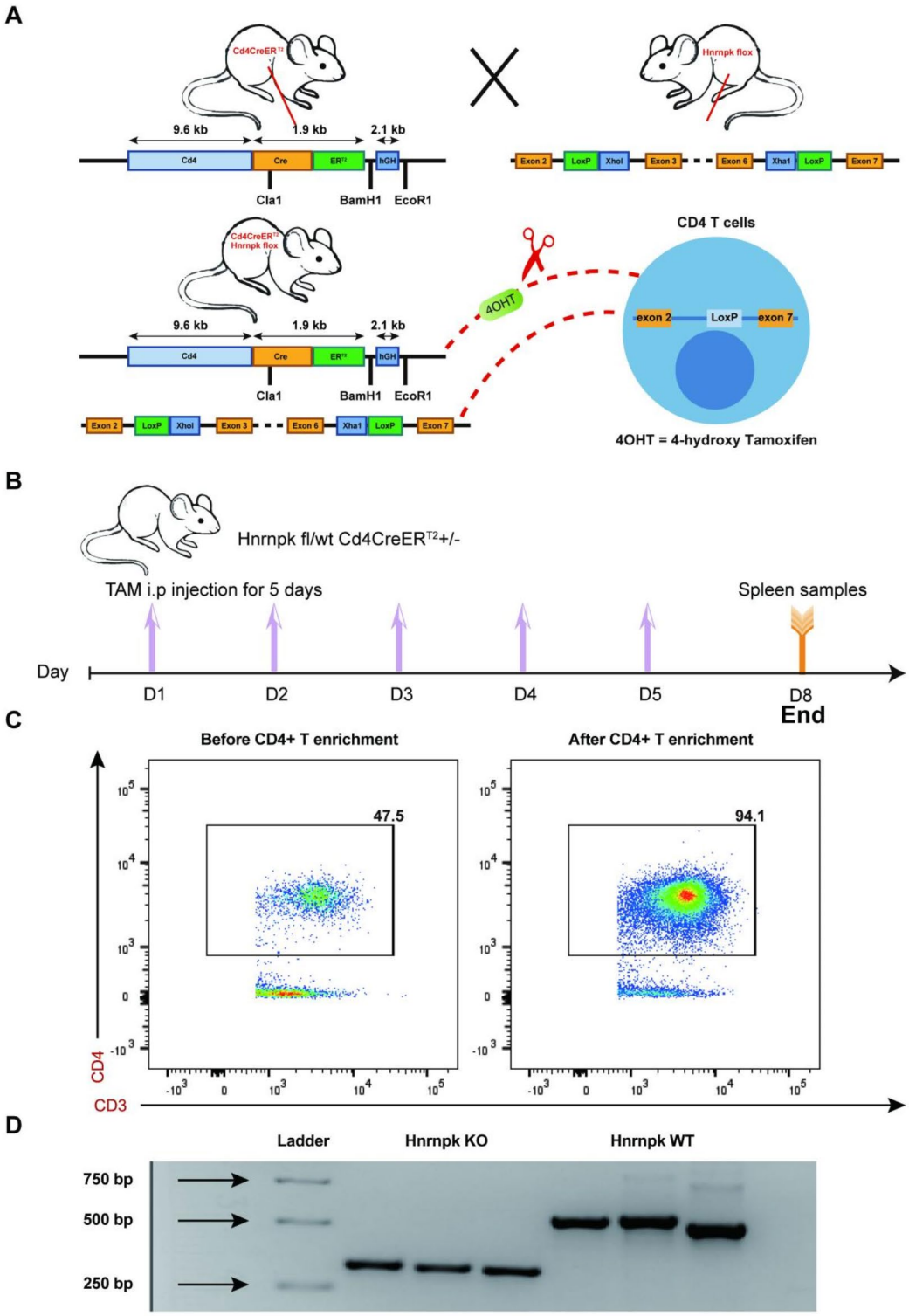

Fig. 2. (**A**) Breeding scheme used to create Hnrnpk flox/wt Cd4CreER^{T2} mouse. (**B**) Schematic diagram illustrating the Hnrnpk knockout using Tamoxifen in Hnrnpk flox/wt Cd4CreER^{T2} mouse. Tamoxifen was administered to mice for 5 continuous days via intraperitoneal injection (i.p.). On day 8, the spleen was collected, and CD4 + T cells were enriched. TAM: tamoxifen, i.p: intraperitoneal. (**C**) Representative flow cytometry plots showing CD3 + CD4 + T cells in splenocytes before and after CD4 + T cell enrichment. (**D**) Agarose gel electrophoresis image displaying the PCR product of recombinant Hnrnpk following Hnrnpk deletion (Hnrnpk KO) using three different sets of primers, and unrecombined Hnrnpk (Hnrnpk WT) also using three different sets of primers. (Original gel is presented in Supplementary Fig. 2).

The flow cytometry results on the splenocytes from another *2 Hnrnpk fl/wt Cd4CreER^{T2}* mice showed Hnrpnk protein level in CD4 + T cells was reduced after tamoxifen injection compared to two *Hnrnpk fl/wt Cd4CreER^{T2}* mice that did not receive tamoxifen (control group). (Supplementary Fig. 3)

3. T-cell infiltration limited to cutaneous region and undisturbed immune homeostasis in peripheral blood in the conditional knockout mice with single-copy *Hnrnpk* deficiency in skin-resident CD4 + T cells.

In this experiment, *Hnrnpk fl/wt Cd4CreER^{T2}* mice were used to induce sustained chronic inflammation in the skin using OXA and topically applied tamoxifen to knock out *Hnrnpk* in CD4 + T cells within the skin. (Fig. 3A) One flank was treated and the collateral flank was left untreated as matched internal control. The specific application of reagents was implemented as previously described[18,19]. From these earlier experiments we know that without tamoxifen (no recombination at floxed sites) the chronic inflammation faded after discontinuation of the allergic challenges to a level observed in untreated flanks in the test animals.

Flow cytometry analysis of peripheral blood during the 40-week experiment showed that repeated topical application of low-concentration OXA did not result in significant abnormalities in immune cell populations. The ratio of CD3 + cells to CD19 + cells in peripheral blood of all mice did not exhibit noticeable fluctuations (Fig. 3B). Similarly, the ratio of CD4 + cells to CD8 + cells in peripheral blood of all mice also did not show significant fluctuations. (Fig. 3C). The ratios of immune cell subpopulations remained relatively stable throughout the experiment.

Flow cytometry analysis showed successful cell extraction from mouse skin, and the proportion of CD4 + and CD8 + cells among CD3 + cells was determined. In the cells extracted from the skin, the percentage of CD4 + cells among CD3 + cells in the left flank (treated flank) was significantly higher compared to the percentage of CD4 + cells among CD3 + cells in the right flank (untreated flank) at a statistically significant level. (Fig. 3D,E). Similarly, the percentage of CD8 + cells among CD3 + cells in the left flank was significantly higher than that of CD8 + cells among CD3 + cells in the right flank. (Fig. 3F,G)

4. Increased skin inflammation with dermal infiltrating lymphocytes, primarily characterized by CD3 + CD4 + cells in transgenic mice with single-copy *Hnrnpk* deficiency in skin-resident CD4 + cells.

In addition to isolation of intact cells from mouse skin, we made sections of paraffin embedded formalin fixed biopsies of mouse skin and performed histopathological analysis using haematoxylin and eosin (H&E) staining and immunohistochemistry (IHC). The H&E staining revealed a minor amount of epidermal cell swelling and lymphocyte infiltration in the dermis of the treated flanks. (Fig. 4A) No significant abnormalities were observed in the epidermis and dermis of the untreated flanks. Quantitative statistical analysis of the epidermal layers showed that the treated flanks exhibited thicker epidermis than the untreated flanks. (Fig. 4A)

Furthermore, we conducted immunohistochemical staining on the mouse skin samples using T-cell (inflammation) markers CD3, CD4, and CD8. The staining results revealed scattered or focal distribution of CD3 + and CD4 + cells in the dermis of the treated flanks, and the presence of CD8 + cells, although with a scattered distribution. In contrast, the untreated flanks showed fewer CD3+, CD4+, and CD8 + lymphocyte infiltrations. (Fig. 4B) Quantitative analysis of CD3+, CD4+, and CD8 + infiltration in the dermis demonstrated a significant increase in the numbers of CD3+, CD4+, and CD8 + cells in the treated flanks compared to the untreated flanks. (Fig. 4B)

Discussion

We established a novel controlled knockout transgenic mouse model to study the function of one-copy loss of *Hnrnpk* in CD4 + T cells. *HNRNPK* has a dual role in tumor suppression and tumor promotion, and its expression may be upregulated or downregulated in different types of tumors. [20,13,21] Previous RNA sequencing studies have shown downregulation of *HNRNPK* expression in CD4 + T cells from patient skin lesions of mycosis fungoides (MF), the most common type of cutaneous T-cell lymphoma (CTCL)[5,22] This abnormality may lead to *HNRNPK* dysfunction, affecting RNA processing and gene expression regulation[23]. Deletions in *HNRNPK* have also been identified in malignant cells from patients with Sézary syndrome (SS) and skin tumor samples from patients with MF[17].

In further validating our *Hnrnpk flox Cd4CreER^{T2}* model, we conducted a comparison with the established *Socs1 flox Cd4CreER^{T2}* transgenic mouse model[19]. The *Socs1 flox Cd4CreER^{T2}* mice serve as targeting skin GEMMs (Genetically Engineered Mouse Models) in CTCL research. Specifically, the inflammatory responses observed following the deletion of *Socs1* in CD4 + T cells suggest that *Socs1* deletion may act as a potential initiator for CTCL[18]. This is similar to our approach in the *Hnrnpk flox Cd4CreER^{T2}* model, where the *Socs1flox Cd4CreER^{T2}* mice employ a targeted gene knockout strategy. This method has effectively simulated the very early characteristics of CTCL, underscoring the relevance and applicability of our technique in studying CTCL pathogenesis. The precision in gene manipulation and the resulting phenotypic manifestations observed in the *Socs1 flox Cd4CreER^{T2}* model lend credibility to the skin painting method and gene knockout technique used in our study.

Thanks to the reporter gene, deletion of the *Socs1* gene in the CD4 + T cells of these hybrid mice can be detected via flow cytometry[24]. In the *Hnrnpk flox Cd4CreER^{T2}* mice, the knockout of *Hnrnpk*, which lacks a reporter gene, is verified by extracting DNA from enriched CD4 + T cells and employing PCR technology. These procedures have effectively confirmed the efficacy of the *Cd4CreER^{T2}* knockout tool.

In the *Socs1 flox Cd4CreER^{T2}* model, deletion of the *Socs1* gene, combined with topical sensitizing stimuli, leads to autonomous skin inflammation exhibiting early MF characteristics. This closely mirrors the conditions observed in early-stage human CTCL[25]. Similarly, in our *Hnrnpk flox Cd4CreER^{T2}* mice, the targeted gene

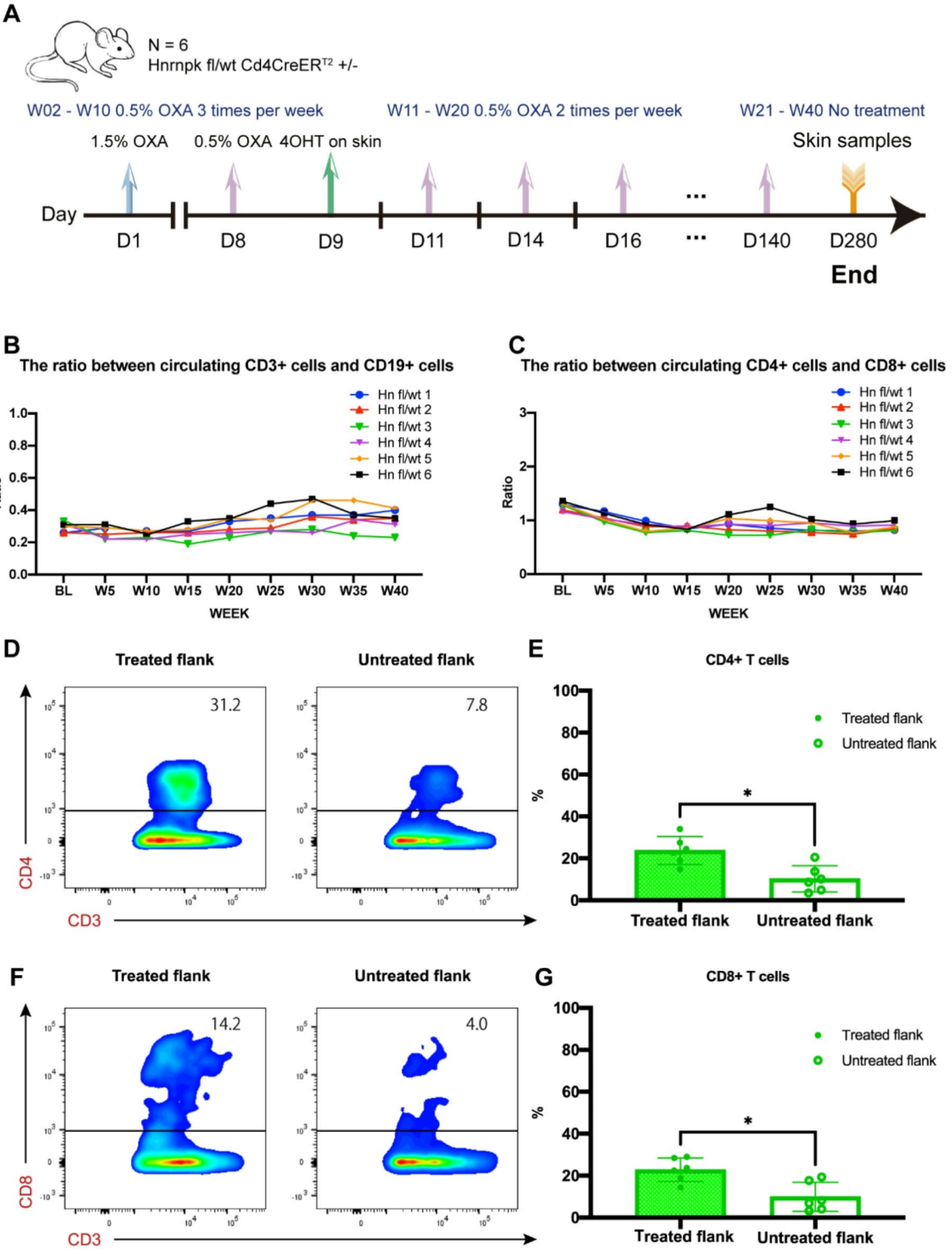

Fig. 3. (**A**) Schematic diagram illustrating the experiment in Hnrnpk flox Cd4CreER^{T2} transgenic mice. D: day, W: week, OXA: oxazolone, 4OHT: 4-hydroxy-tamoxifen. Blood collection was performed 24 h after OXA application. Skin samples were collected at the end of the experiment. (**B**, **C**) Overview of the ratio between CD3 + cells and CD19 + cells, and between CD4 + cells and CD8 + cells in peripheral blood throughout the experiment. (**D**, **E**) Representative flow cytometry plots and quantitative analysis of CD3 + CD4 + T cells in treated and untreated flanks. $P = 0.0159$. (**F**, **G**) Representative flow cytometry plots and quantitative analysis of CD3 + CD8 + T cells in treated and untreated flanks. $P = 0.0111$. The data were presented as means ± SDs. Statistical analysis was performed using a pair t-test. Differences were considered statistically significant when $P < 0.05$ ($^*p < 0.05$).

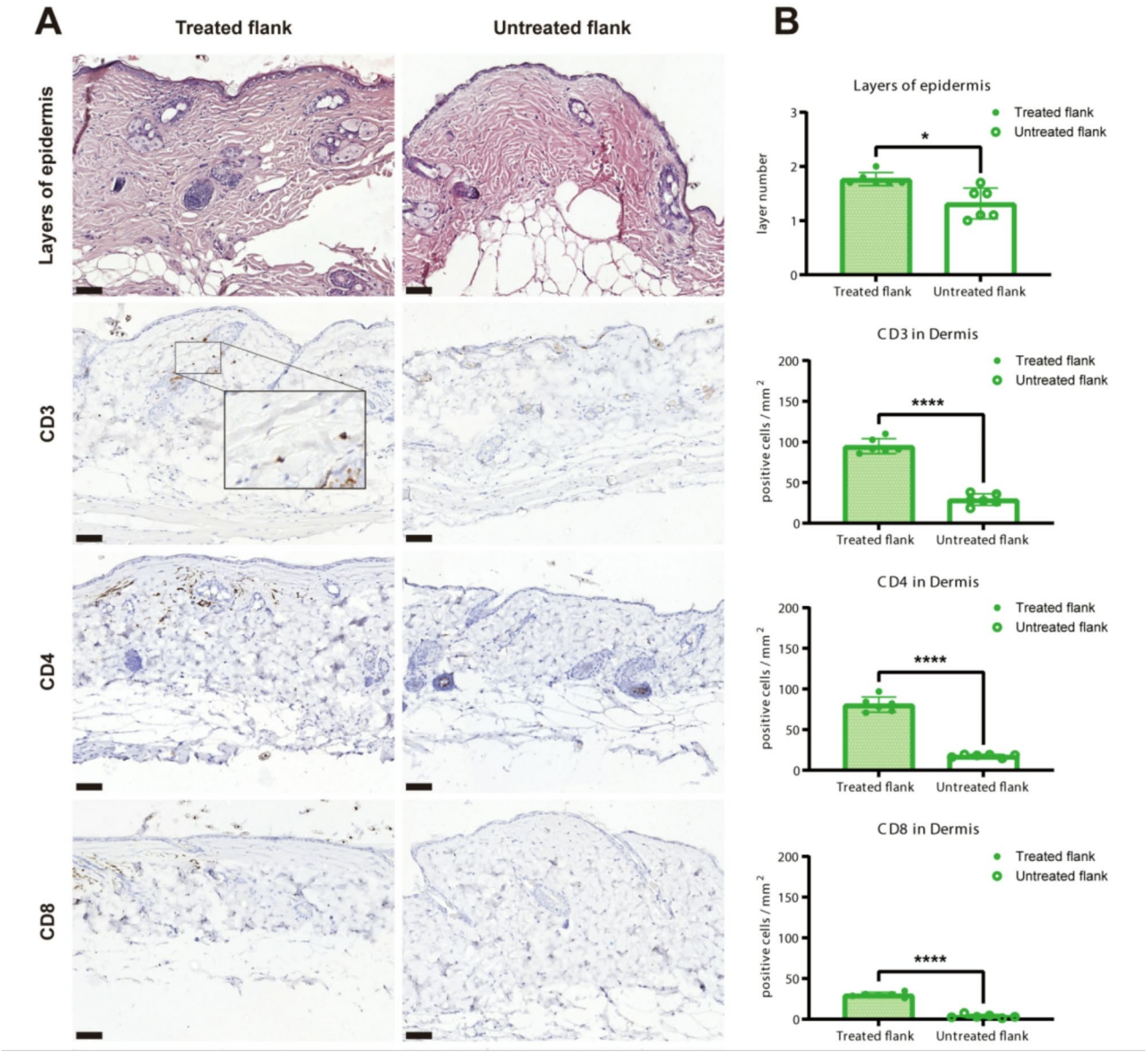

Fig. 4. (**A**) Representative HE staining images and immunohistochemistry staining images of CD3, CD4 and CD8 in treated flanks and untreated flanks. (**B**) Quantitative analysis of the layer numbers of epidermis ($P = 0.0312$) and the quantitative analysis of CD3 ($P = 0.000052$), CD4 ($P = 0.000019$) and CD8 ($P = 0.000002$). The results were obtained by counting within five high-power fields (HPFs) at 20x magnification for each slide, with the mean values displayed in the figure. Scale bar = 50 μm. The data were presented as means ± SDs. A paired t-test or non-parametric test was used. A p-value of 0.05 or below was considered significant (*) and $p < 0.0001$ (****) was considered highly significant.

knockout resulted in a phenotype that accurately reflects early CTCL characteristics, particularly in early-stage MF. This similarity not only validates our methodological approach but also significantly enhances the potential of our model in revealing new insights into the molecular basis of CTCL. The ability to precisely knockout genes of interest, as demonstrated in both the *Socs1 flox Cd4CreER*^{T2} and our *Hnrnpk flox Cd4CreER*^{T2} models, is crucial for dissecting the complex interplay of genetic factors in the pathogenesis and progression of CTCL.

Our novel mouse model shows no significant disturbances in the immune cell population in peripheral blood, aligning with the localized nature of MF in CTCL and the challenge of distinguishing benign and malignant T cells in early-stage MF skin lesions[4,8]. In our new mouse model, skin inflammation persists even after the stimulus is removed, indicating a sustained chronic inflammatory response locally. However, there were no significant disturbances observed in the immune cell population in the peripheral blood. This pattern aligns with the early manifestations of mycosis fungoides (MF) in cutaneous T-cell lymphoma (CTCL), characterized by long-lasting and persistent inflammation limited to the skin[2,26] Most MF patients also suffer from localized

skin diseases, and distinguishing between benign and malignant T cells in early-stage MF lesions is challenging due to their shared T-cell characteristics and overlapping phenotypes[27].

CTCL involves the coexistence of malignant CD4 + T cells, secreting cytokines, and normal tissue-resident memory T cells (TRM cells) that also contribute to the complex microenvironment through cytokine secretion[28]. CTCL cells, and CD4 + TRM cells, share a common tissue differentiation program likely influenced by the skin microenvironment[29]. In our mouse model, dermal infiltrating lymphocytes in *Hnrnpk* knockout mice primarily consisted of CD3 + CD4 + cells, mirroring the lymphocyte profile seen in human CTCL skin lesions. The increase in CD8 + T cells was less pronounced, suggesting an expansion of cytotoxic CD8 + T cells followed by gradual depletion.

Next to introducing the new mutant mouse model in this study, several limitations need to be addressed. The first limitation is the sample size of mice in long-term experiments. Additionally, further investigations are needed to validate the findings from sequencing studies in CTCL patients and explore the role of *HNRNPK* deletion in CTCL development and progression.

In conclusion, we established a novel genetically modified mouse model with conditional *Hnrnpk* knockout specifically in CD4 + T cells to investigate its role in CTCL pathogenesis. This model exhibits features consistent with CTCL, such as chronic skin inflammation, lymphocytic infiltration predominantly composed of CD3 + CD4 + cells. Our work provides insights into the mechanisms underlying CTCL progression and validates findings from sequencing studies in CTCL patients. Future mouse studies with larger sample sizes and longer follow-up are necessary to further enhance our understanding of *HNRNPK* involvement in CTCL.

Materials and methods

Ethical statement

All mouse experiments were supervised by the animal welfare committee (IvD) of the Leiden University Medical Center and approved by the national central committee of animal experiments (CCD) under the permit number AVD116002015271, in accordance with the Dutch Act on Animal Experimentation and EU Directive 2020/63/EU. The study is reported in accordance with the ARRIVE guidelines.

Animals

Hnrnpk flox (*Hnrnpk*^{em1Lumc}; MGI:99894) mice where loxP sites were introduced in *Hnrnpk* intron 2 and intron 6 were generated at LUMC. *Hnrnpk* flox mice using CrisprCas9 RNP and 200 bp single-stranded oligodeoxynucleotides (ssODN). (all from IDT) *Cd4CreER*^{T2} mice (Tg (Cd4-cre/ER^{T2})11Gnri/J; MGI:5493114; JAX:022356) expressing CreER^{T2} recombinase under the control of the Cd4 promoter were purchased from The Jackson Laboratory (JAX). *Hnrnpk* flox mice were mated with *Cd4CreER*^{T2} mice to generate *Hnrnpk flox Cd4CreER*^{T2} mice. The offspring inherited both the targeted *Hnrnpk flox* allele and the *Cd4CreER*^{T2} transgenes.

Male *Hnrnpk flox/wt Cd4CreER*^{T2} + mice, 12–15 weeks old, were housed in a temperature-controlled room with a 12-hour light-dark cycle. Throughout the experiment, food and tap water were available *ad libitum*.

Tamoxifen and oxazolone application

Tamoxifen (TAM, Sigma-Aldrich, Netherlands) was dissolved in peanut oil at a concentration of 10 mg/ml, and 4-hydroxy-Tamoxifen (4OHT, Sigma-Aldrich, Netherlands) was dissolved in ethanol (20 mg/ml) and sonicated for 2 min. Tamoxifen was administered at a dose of 1 mg per mouse per day by intraperitoneal injection for 5 consecutive days. 4OHT was topically administered at a dose of 1 mg per mouse on the left shaved skin (2 cm × 3 cm). Oxazolone (4-Ethoxymethylene-2-phenyl-2-oxazolin-5-one, Sigma-Aldrich, Netherlands) was dissolved in acetone. A freshly made solution of oxazolone was used for each experiment. The application schedule was as follows:

On the first day, 1.5% OXA (100 µl) was applied to the abdomen for induction. On the eighth day, 0.5% OXA (150 µl) was applied to the left flank. On the ninth day, the CRE-Lox system was activated with 4OHT to knock out *Hnrnpk* in CD4 + T cells. From week 2 to week 10, 0.5% OXA was applied three times per week to the left flank. From week 11 to week 20, 0.5% OXA was applied twice per week to the left flank. From week 21 to week 40, the mice were monitored for their overall condition, particularly their skin condition. The corresponding right flank was used as the control using the vehicle only.

Peripheral blood samples were collected from mice via the tail vein weekly or biweekly, and flow cytometry was performed to analyze the immune cell populations in the peripheral blood. At the end of week 40, all mice were humanely euthanized by carbon dioxide inhalation and skin specimens were collected from both the left and right flanks of the mice for cell extraction and preparation of paraffin-embedded sections.

Cell isolation and DNA isolation

Intact skin cells were isolated by taking a 4 mm skin biopsy, which was then digested using the whole skin dissociation Kit (Miltenyi Biotec, NL) following the manufacturer's instructions. CD4 + T splenocytes were isolated and enriched by processing the spleen using lysis buffer (from Hospital Pharmacy at LUMC) to obtain splenocytes. CD4 + T cells were enriched from the splenocyte suspension using The BD IMag™ Mouse CD4 + T Lymphocyte Enrichment Set (BD Biosciences, NL). DNA was isolated from ear-clips and the CD4 + T cells from splenocytes using DNeasy Blood & Tissue Kits (Qiagen, NL).

Genomic PCR was conducted to analyze the genotypes of mice using ear DNA and gene-specific primers (Table S1) for the *Hnrnpk* flox transgene and *Hnrnpk* wildtype gene. Genomic PCR was conducted on the DNA from enriched CD4 + splenoctyes to detect the recombinant *Hnrnpk* transgene and unrecombined *Hnrnpk* wildtype gene using the three different sets of gene-specific primers respectively (Table S2).

Flow cytometry

Samples from isolated skin cells, splenocytes before and after CD4 + T cell enrichment, and blood were used for flow cytometry. Blood samples were handled and stained as described previously[18]. Fluorescence-labelled antibodies, including Live/Dead marker (clone Zombie, BD, Netherlands), anti-mouse CD3 (clone 145-2C11, BD, Netherlands), anti-mouse CD19 (clone 1D3, Thermo Fisher Scientific, Netherlands), anti-mouse CD4 (clone RM4-5, Thermo Fisher Scientific, Netherlands), anti-mouse CD8 (clone 53 – 6.7, Biolegend, Netherlands), CD4 AlexaFluor647 (ThermoFisher, cat: 51-0042-82), HNRNPK (ThermoFisher, cat 11426-1-AP) and anti-Goat secondary AlexaFluor488 (ThermoFisher, cat A-11034), were used. Samples were processed in a BD Fortessa and Cytek Biosciences Aurora flow cytometer. The raw data were analyzed using FlowJo or Infinicyt software and median fluorescence intensity of *Hnrnpk* was analyzed.

Histological and immunohistochemical analyses

Skin samples were fixed with 4% paraformaldehyde, dehydrated, and paraffin-embedded. Section (4 µm-thick) were cut with a microtome (Leica 149MULTI0C1). Tissue sections were stained with hematoxylin and eosin. For immunohistochemistry analyses, tissue sections were deparaffinized, rehydrated, and blocked for endogenous peroxidase using 0.3% hydrogen peroxide and nonspecific antibody binding using a blocking buffer (SuperBlock, Thermo Fisher Scientific, The Netherlands). Antigen retrieval was performed using citric acid (pH 6.0) solution. The tissue sections were incubated with the following primary antibodies at 4 °C overnight: anti-mouse CD3 (1:200, D7A6E, Cell Signaling Technology, Netherlands), anti-mouse CD4 (1:100, D7D2Z, Cell Signaling Technology, Netherlands), anti-mouse CD8 (1:1600, 4SM15, eBioscience™, Netherlands). Then, sections were incubated with secondary antibodies at room temperature for 60 min. Sections were visualized with the Vectastain Elite Kit (Vector Labs, Netherlands) and diaminobenzidine (Dako Omnis, Agilent Dako, Netherlands). After counterstaining with hematoxylin, sections were mounted. The scanner (3DHISTECH, Pannoramic 250) was used for microscopic examination and image acquisition.

The layers of the epidermis were counted within 5 high-power fields (HPF) (20x magnification) of each slide, and the mean values were calculated for subsequent statistical analysis. The numbers of CD3+, CD4+, and CD8 + lymphocytes in the dermis were counted within 5 HPF (20x magnification) per case. The values were normalized to cells/mm2, and the mean numbers were assessed for further statistical analysis. The evaluations were conducted by two independent individuals who were blinded to sample information.

Statistical analysis

Statistical analysis was performed using GraphPad Prism software (version 8.0.1). A paired t-test was used to compare the treated flank and untreated flank in mice. A p-value of 0.05 or below was considered significant (*), $p < 0.01$ (**), $p < 0.001$ (***) and $P < 0.0001$ (****) was considered highly significant.

Data availability

The sequences generated are available in the EU Open Research Repository zenodo repository https://zenodo.org/records/15191320, and the original images used in this study are available in the supplementary files. All other data are available from the corresponding author upon reasonable request.

Received: 16 February 2024; Accepted: 14 April 2025
Published online: 24 April 2025

References

1. Willemze, R. Primary cutaneous lymphoma: the 2018 update of the WHO-EORTC classification. *Presse Med.* **51**, 104126. https://doi.org/10.1016/j.lpm.2022.104126 (2022).
2. Rein Willemze, L. C., Kempf, W., Swerdlow, S. H., Elaine, S. & Jaffe Emilio Berti, Fabio Facchetti, 5, and The 2018 update of the WHO-EORTC classification for primary cutaneous lymphomas. *Blood* (2018).
3. Tensen, C. P., Quint, K. D. & Vermeer, M. H. Genetic and epigenetic insights into cutaneous T-cell lymphoma. *Blood* **139**, 15–33. https://doi.org/10.1182/blood.2019004256 (2022).
4. Ren, J. et al. Integrated transcriptome and trajectory analysis of cutaneous T-cell lymphoma identifies putative precancer populations. *Blood Adv.* **7**, 445–457. https://doi.org/10.1182/bloodadvances.2022008168 (2023).
5. Bastidas Torres, A. N. et al. Genomic analysis reveals recurrent deletion of JAK-STAT signaling inhibitors HNRNPK and SOCS1 in mycosis fungoides. *Genes Chromosomes Cancer*. **57**, 653–664. https://doi.org/10.1002/gcc.22679 (2018).
6. Gill, R. P. K. et al. Understanding cell lines, Patient-Derived xenograft and genetically engineered mouse models used to study cutaneous T-Cell lymphoma. *Cells* **11** https://doi.org/10.3390/cells11040593 (2022).
7. Kalliara, E., Belfrage, E., Gullberg, U., Drott, K. & Ek, S. Spatially guided and single cell tools to map the microenvironment in cutaneous T-Cell lymphoma. *Cancers (Basel)*. 15. https://doi.org/10.3390/cancers15082362 (2023).
8. Han, Z. et al. MicroRNA Regulation of T-cell exhaustion in cutaneous T cell lymphoma. *J Invest Dermatol* 142, 603–612 e607, (2022). https://doi.org/10.1016/j.jid.2021.08.447
9. Trochopoulos, A. G. X. et al. Micellar curcumin substantially increases the antineoplastic activity of the alkylphosphocholine erufosine against TWIST1 positive cutaneous T cell lymphoma cell lines. *Pharmaceutics* 14, (2022). https://doi.org/10.3390/pharmaceutics14122688
10. Patil, K. et al. Molecular pathogenesis of cutaneous T cell lymphoma: Role of chemokines, cytokines, and dysregulated signaling pathways. *Semin Cancer Biol.* **86**, 382–399. https://doi.org/10.1016/j.semcancer.2021.12.003 (2022).
11. Barboro, P., Ferrari, N. & Balbi, C. Emerging roles of heterogeneous nuclear ribonucleoprotein K (hnRNP K) in cancer progression. *Cancer Lett.* **352**, 152–159. https://doi.org/10.1016/j.canlet.2014.06.019 (2014).
12. Mucha, B. et al. Tumor suppressor mediated ubiquitylation of HnRNPK is a barrier to oncogenic translation. *Nat. Commun.* **13**, 6614. https://doi.org/10.1038/s41467-022-34402-6 (2022).
13. Gallardo, M. et al. Aberrant HnRNP K expression: all roads lead to cancer. *Cell. Cycle.* **15**, 1552–1557. https://doi.org/10.1080/15384101.2016.1164372 (2016).
14. Naarmann-de Vries, I. S. et al. Characterization of acute myeloid leukemia with del(9q) - Impact of the genes in the minimally deleted region. *Leuk. Res.* **76**, 15–23. https://doi.org/10.1016/j.leukres.2018.11.007 (2019).

15. Dayyani, F. et al. Loss of TLE1 and TLE4 from the del(9q) commonly deleted region in AML cooperates with AML1-ETO to affect myeloid cell proliferation and survival. *Blood* **111**, 4338–4347. https://doi.org/10.1182/blood-2007-07-103291 (2008).
16. Gallardo, M. et al. HnRNP K is a haploinsufficient tumor suppressor that regulates proliferation and differentiation programs in hematologic malignancies. *Cancer Cell.* **28**, 486–499. https://doi.org/10.1016/j.ccell.2015.09.001 (2015).
17. Park, J., Daniels, J., Wartewig, T., Ringbloom, K. G., Martinez-Escala, M. E., Choi,S., Thomas, J. J., Doukas, P. G., Yang, J., Snowden, C., Law, C., Lee, Y., Lee, K.,Zhang, Y., Conran, C., Tegtmeyer, K., Mo, S. H., Pease, D. R., Jothishankar, B., Kwok, P. Choi, J. Integrated genomic analyses of cutaneous T-cell lymphomas reveal the molecular bases for disease heterogeneity. *Blood*, https://doi.org/10.1182/blood.2020009655 (2021).
18. Luo, Y., de Haan, V. M., Kinderman, S., de Gruijl, P. & van Hall, F. R. Socs1-knockout in skin-resident CD4(+) T cells in a protracted contact-allergic reaction results in an autonomous skin inflammation with features of early-stage mycosis fungoides. *Biochem. Biophys. Rep.* **35**, 101535. https://doi.org/10.1016/j.bbrep.2023.101535 (2023).
19. Luo, Y. et al. In vivo modelling of cutaneous T-cell lymphoma: The role of SOCS1. *Front. Oncol.* **12**, 1031052. https://doi.org/10.3389/fonc.2022.1031052 (2022).
20. Wang, Z., He, Q. H., Liu, J., Xue, L. & Fox, W. The emerging roles of HnRNPK. *J. Cell. Physiol.* **235**, 1995–2008. https://doi.org/10.1002/jcp.29186 (2020).
21. Chen, Y., Xiao, Z. Y., Chen, Z., Li, S. & Zou, Y. Role of heterogeneous nuclear ribonucleoprotein K in tumor development. *J. Cell. Biochem.* **120**, 14296–14305. https://doi.org/10.1002/jcb.28867 (2019).
22. Fan, X. et al. Cytoplasmic HnRNPK interacts with GSK3beta and is essential for the osteoclast differentiation. *Sci. Rep.* **5**, 17732. https://doi.org/10.1038/srep17732 (2015).
23. Xu, Y. et al. New insights into the interplay between Non-Coding RNAs and RNA-Binding protein HnRNPK in regulating cellular functions. *Cells* **8** https://doi.org/10.3390/cells8010062 (2019).
24. Aghajani, K., Keerthivasan, S., Yu, Y. & Gounari, F. Generation of CD4CreER(T(2)) Transgenic mice to study development of peripheral CD4-T-cells. *Genesis* **50**, 908–913. https://doi.org/10.1002/dvg.22052 (2012).
25. Krejsgaard, T. et al. Malignant inflammation in cutaneous T-cell lymphoma-a hostile takeover. *Semin Immunopathol.* **39**, 269–282. https://doi.org/10.1007/s00281-016-0594-9 (2017).
26. Vieyra-Garcia, P. et al. Benign T cells drive clinical skin inflammation in cutaneous T cell lymphoma. *JCI Insight*. **4** https://doi.org/10.1172/jci.insight.124233 (2019).
27. Roediger, B. & Schlapbach, C. T cells in the skin: lymphoma and inflammatory skin disease. *J. Allergy Clin. Immunol.* **149**, 1172–1184. https://doi.org/10.1016/j.jaci.2022.02.015 (2022).
28. Stolearenco, V. et al. Cellular interactions and inflammation in the pathogenesis of cutaneous T-Cell lymphoma. *Front. Cell. Dev. Biol.* **8**, 851. https://doi.org/10.3389/fcell.2020.00851 (2020).
29. Bertschi, N. L., Bazzini, C. & Schlapbach, C. The concept of pathogenic TH2 cells: collegium internationale allergologicum update 2021. *Int. Arch. Allergy Immunol.* **182**, 365–380. https://doi.org/10.1159/000515144 (2021).

Acknowledgements

We would like to thank Roos Gaarkeuken and Yang Liu for technical assistance. We thank the Animal Facility of the Leiden University Medical Center (LUMC) for their excellent care of the animals and the Flow cytometry Core Facility of Leiden University Medical Center (LUMC) for their support.

Author contributions

Conceptualization: CPT and MV. Methodology: CPT, FRG, YL, MML, PH, FJB and MPV. Data curation: YL, MML, CB, JC, PH, FJB and MPV. Formal analysis: YL, MML, CB, JC, FJB, FRG and CPT. Writing - Original Draft Preparation: YL. Writing - Review and Editing: CPT, YL, MML, CB, JC, FRG, PH, FJB and MPV. All authors have read and agreed to the published version of the manuscript.

Declarations

Competing interest

The authors declare no competing interests.

Human and animal rights

Hnrnpk flox (*Hnrnpk*^{em1Lumc}; MGI:99894) mice were generated at Leiden University Medical Center (LUMC). *Cd4CreER*^{T2} mice (Tg(Cd4-cre/ER^{T2})11Gnri/J; MGI:5493114; JAX:022356) were purchased from The Jackson Laboratory (JAX).

Additional information

Supplementary Information The online version contains supplementary material available at https://doi.org/10.1038/s41598-025-98640-6.

Correspondence and requests for materials should be addressed to C.P.T.